Unforeseen plant phenotypic diversity in a dry and grazed world

Nicolas Gross, Fernando Maestre, Pierre Liancourt, Miguel Berdugo, Raphaël Martin, Beatriz Gozalo, Victoria Ochoa, Manuel Delgado-Baquerizo, Vincent Maire, Hugo Saiz, et al.

Unforeseen plant phenotypic diversity in a dry and grazed world

Nicolas Gross[1,*], Fernando T. Maestre[2], Pierre Liancourt[3,4], Miguel Berdugo[5,6], Raphaël Martin[1], Beatriz Gozalo[7], Victoria Ochoa[7], Manuel Delgado-Baquerizo[8], Vincent Maire[9], Hugo Saiz[10], Santiago Soliveres[7,11], Enrique Valencia[5], David J. Eldridge[12], Emilio Guirado[7], Franck Jabot[1], Sergio Asensio[7], Juan J. Gaitán[13,14,15], Miguel García-Gómez[16], Paloma Martínez[17], Jaime Martínez-Valderrama[7], Betty J. Mendoza[18], Eduardo Moreno-Jiménez[19], David S. Pescador[18,20], César Plaza[17], Ivan Santaolaria Pijuan[7], Mehdi Abedi[21], Rodrigo J. Ahumada[22], Fateh Amghar[23], Antonio I. Arroyo[24], Khadijeh Bahalkeh[21], Lydia Bailey[25], Farah Ben Salem[26], Niels Blaum[27], Bazartseren Boldgiv[28], Matthew A. Bowker[25,29], Cristina Branquinho[30], Liesbeth van den Brink[4,31], Chongfeng Bu[32,33], Rafaella Canessa[4,34,35], Andrea del P. Castillo-Monroy[36], Helena Castro[37], Patricio Castro[38], Roukaya Chibani[39], Abel Augusto Conceição[40], Anthony Darrouzet-Nardi[41], Yvonne C. Davila[42], Balázs Deák[43], David A. Donoso[36], Jorge Durán[44], Carlos Espinosa[45], Alex Fajardo[46,47,48], Mohammad Farzam[49], Daniela Ferrante[50,51], Jorgelina Franzese[52], Lauchlan Fraser[53], Sofía Gonzalez[52], Elizabeth Gusman-Montalvan[45], Rosa Mary Hernández-Hernández[54], Norbert Hölzel[55], Elisabeth Huber-Sannwald[56], Oswaldo Jadan[38], Florian Jeltsch[27], Anke Jentsch[57], Mengchen Ju[32,33], Kudzai F. Kaseke[58], Liana Kindermann[59], Peter le Roux[60], Anja Linstädter[59,61], Michelle A. Louw[60], Mancha Mabaso[62], Gillian Maggs-Kölling[63], Thulani P. Makhalanyane[64], Oumarou Malam Issa[65], Antonio J. Manzaneda[66], Eugene Marais[63], Pierre Margerie[67], Frederic Mendes Hughes[40,68,69], João Vitor S. Messeder[70], Juan P. Mora[46], Gerardo Moreno[71], Seth M. Munson[72], Alice Nunes[30], Gabriel Oliva[50,51], Gaston R. Oñatibia[73], Guadalupe Peter[15,74], Yolanda Pueyo[24], R. Emiliano Quiroga[22,75], Elizabeth Ramírez-Iglesias[76], Sasha C. Reed[77], Pedro J. Rey[78], Víctor M. Reyes Gómez[79], Alexandra Rodríguez[44], Victor Rolo[71], Juan G. Rubalcaba[5], Jan C. Ruppert[4], Osvaldo Sala[80], Ayman Salah[81], Phokgedi Julius Sebei[82], Ilan Stavi[83], Colton Stephens[53], Alberto L. Teixido[5], Andrew D. Thomas[84], Heather L. Throop[85,86], Katja Tielbörger[4], Samantha Travers[87], Sainbileg Undrakhbold[28], James Val[87], Orsolya Valkó[43], Frederike Velbert[55], Wanyoike Wamiti[88], Lixin Wang[89], Deli Wang[90], Glenda M. Wardle[91], Peter Wolff[57], Laura Yahdjian[73], Reza Yari[92], Eli Zaady[93], Juan Manuel Zeberio[74], Yuanling Zhang[94], Xiaobing Zhou[94], Yoann Le Bagousse-Pinguet[95]

*Corresponding author: nicolas.gross@inrae.fr

Author's affiliations

[1] Université Clermont Auvergne, INRAE, VetAgro Sup, Unité Mixte de Recherche Ecosystème Prairial; Clermont-Ferrand, France

[2] Environmental Sciences and Engineering, Biological and Environmental Science and Engineering Division, King Abdullah University of Science and Technology, Thuwal, 23955-6900, Kingdom of Saudi Arabia

[3] Institute Botany Department. State Museum of Natural History Stuttgart; Stuttgart, Germany

[4] Plant Ecology Group, University of Tübingen, Tübingen, Germany

[5] Departamento de Biodiversidad, Ecología y Evolución, Facultad de Ciencias Biológicas, Universidad Complutense de Madrid, 28040, Madrid, Spain

[6] Department of Environmental Systems Science, ETH Zurich; Zurich, Switzerland

[7] Instituto Multidisciplinar para el Estudio del Medio "Ramon Margalef", Universidad de Alicante, Alicante, Spain

[8] Laboratorio de Biodiversidad y Funcionamiento Ecosistémico. Instituto de Recursos Naturales y Agrobiología de Sevilla (IRNAS), CSIC; Sevilla, Spain

[9] Département des sciences de l'environnement, Université du Québec à Trois-Rivières, Trois Rivières, Canada

[10] Departamento de Ciencias Agrarias y Medio Natural, Escuela Politécnica Superior, Instituto Universitario de Investigación en Ciencias Ambientales de Aragón (IUCA), Universidad de Zaragoza, Huesca, Spain

[11] Departamento de Ecología, Universidad de Alicante, Alicante, Spain

[12] Centre for Ecosystem Science, School of Biological, Earth and Environmental Sciences, University of New South Wales; Sydney, Australia

[13] Instituto Nacional de Tecnología Agropecuaria (INTA), Instituto de Suelos-CNIA; Buenos Aires, Argentina

[14] Universidad Nacional de Luján, Departamento de Tecnología; Luján, Argentina

[15] Consejo Nacional de Investigaciones Científicas y Técnicas de Argentina (CONICET); Buenos Aires, Argentina

[16] Departamento de Ingeniería y Morfología del Terreno, Escuela Técnica Superior de Ingenieros de Caminos, Canales y Puertos, Universidad Politécnica de Madrid; Madrid, Spain

[17] Instituto de Ciencias Agrarias, Consejo Superior de Investigaciones Científicas; Madrid, Spain

[18] Departamento de Biología y Geología, Física y Química Inorgánica, Universidad Rey Juan Carlos; Móstoles, Spain

[19] Department of Agricultural and Food Chemistry, Faculty of Sciences, Universidad Autónoma de Madrid; Madrid, Spain.

[20] Departamento de Farmacología, Farmacognosia y Botánica, Facultad de Farmacia, Universidad Complutense de Madrid; Madrid, Spain

[21] Department of Range Management, Faculty of Natural Resources and Marine Sciences, Tarbiat Modares University; Noor, Mazandaran Province, I. R. Iran

[22] Instituto Nacional de Tecnología Agropecuaria, Estación Experimental Agropecuaria Catamarca, Catamarca, Argentina

[23] Laboratoire de Recherche: Biodiversité, Biotechnologie, Environnement et Développement Durable (BioDev), Faculté des Sciences, Université M'hamed Bougara de Boumerdès; Boumerdès, Algérie

[24] Instituto Pirenaico de Ecología (IPE, CSIC) Montañana Avenue 1005, 50159, Zaragoza, Spain

[25] Center for Ecosystem Science and Society, Northern Arizona University, Flagstaff, AZ, USA

[26] Laboratory of pastoral ecosystems and promotion of spontaneous plants and associated micro-organisms, Institut des Régions Arides (IRA) Médenine, University of Gabes, Tunisia

[27] University of Potsdam, Plant Ecology & Nature Conservation, Am Mühlenberg 3, 14476 Potsdam

[28] Department of Biology, School of Arts and Sciences, National University of Mongolia, Ulaanbaatar 14201, Mongolia

[29] School of Forestry, Northern Arizona University, Flagstaff, AZ, USA.

[30] cE3c - Centre for Ecology, Evolution and Environmental Changes & CHANGE – Global Change and Sustainability Institute, Faculdade de Ciências, Universidade de Lisboa, 1749-016 Lisboa, Portugal

[31] ECOBIOSIS, Departmento of Botánica, Universidad de Concepción, Chile

[32] Institute of Soil and Water Conservation, Northwest A & F University; Yangling, Shaanxi, China

[33] Institute of Soil and Water Conservation, Chinese Academy of Sciences and Ministry of Water Resources; Yangling, Shaanxi, China

[34] German Centre for Integrative Biodiversity Research (iDiv) Halle-Jena-Leipzig, Puschstrasse 4, 04103 Leipzig, Germany

[35] Institut für Biologie, Martin-Luther-University Halle-Wittenberg, Halle, Germany

[36] Departamento de Biología, Escuela Politécnica Nacional, Quito, Ecuador

[37] University of Coimbra, Centre for Functional Ecology, Department of Life Sciences; Coimbra, Portugal

[38] Universidad de Cuenca, Facultad de Ciencias Agropecuarias, Carrera de Ingeniería Agronómica, Grupo de Agroforestería, Manejo y Conservación del paisaje, Cuenca, Ecuador

[39] Laboratory of Eremology and combating desertification, Institut des Régions Arides (IRA) Médenine, University of Gabes, Tunisia

[40] Departamento de Ciências Biológicas da Universidade Estadual de Feira de Santana, Bahia, Brasil

[41] Department of Biological Sciences, University of Texas at El Paso; El Paso, TX, USA.

[42] Faculty of Science, University of Technology Sydney, Sydney New South Wales 2007, Australia

[43] Lendület' Seed Ecology Research Group, Institute of Ecology and Botany, Centre for Ecological Research, 2-4 Alkotmány street, H-2163 Vácrátót, Hungary

[44] Misión Biolóxica de Galicia, CSIC; Pontevedra, Spain

[45] Departamento de Ciencias Biológicas y Agropecuarias. Universidad Técnica Particular de Loja, Ecuador

[46] Instituto de Investigación Interdisciplinaria (I3), Vicerrectoría Académica, Universidad de Talca, Chile

[47] Instituto de Ecología y Biodiversidad (IEB), Las Palmeras 3425, Santiago, Chile

[48] Instituto Milenio, Limits of Life (LiLi), Valdivia, Chile

[49] Department of Range and Watershed Management, Faculty of Natural Resources and Environment, Ferdowsi University of Mashhad, Mashhad, Iran.

[50] Instituto Nacional de Tecnología Agropecuaria EEA Santa Cruz; Río Gallegos, Santa Cruz, Argentina

[51] Universidad Nacional de la Patagonia Austral; Río Gallegos, Santa Cruz, Argentina

[52] Instituto de Investigaciones en Biodiversidad y Medioambiente (Consejo Nacional de Investigaciones Científicas y Técnicas-Universidad Nacional del Comahue), Argentina

[53] Department of Natural Resource Science, Thompson Rivers University; British Columbia, Canada

[54] Universidad Nacional Experimental Simón Rodríguez (UNESR), Instituto de Estudios Científicos y Tecnológicos (IDECYT); Centro de Estudios de Agroecología Tropical (CEDAT); Miranda, Venezuela

[55] Institute of Landscape Ecology, University of Münster; Münster, Germany

[56] Instituto Potosino de Investigación Científica y Tecnológica, A.C.; San Luis Potosí, México

[57] Department of Disturbance Ecology, Bayreuth Center of Ecology and Environmental Research BayCEER, University of Bayreuth; Bayreuth, Germany

[58] Kudzai F. Kaseke, Earth Research Institute, University of California Santa Barbara, CA 93106, USA

[59] Biodiversity Research/ Systematic Botany Group, Institute of Biochemistry and Biology, University of Potsdam; Potsdam, Germany

[60] Department of Plant and Soil Sciences, University of Pretoria; Pretoria, South Africa

[61] Institute of Crop Science and Resource Conservation, University of Bonn; Bonn, Germany

[62] Department of Biochemistry, Genetics and Microbiology, DSI/NRF SARChI in Marine Microbiomics, University of Pretoria, Hatfield, Lynnwood Road, Pretoria, South Africa

[63] Gobabeb-Namib Research Institute, Walvis Bay, Namibia

[64] Department of Microbiology, Faculty of Science, Stellenbosch University, Stellenbosch, South Africa.

[65] Institut d'Écologie et des Sciences de l'Environnement de Paris (iEES-Paris), Sorbonne Université, IRD, CNRS, INRAE, Université Paris Est Creteil, Université de Paris, Centre IRD de France Nord; Bondy, France

[66] Dept. Biología Animal, Biología Vegetal y Ecología. Universidad de Jaén

[67] Normandie Univ, UNIROUEN, INRAE, ECODIV, 76000 Rouen, France.

[68] Programa de Pós-graduação em Zoologia and Conselho de Curadores das Coleções Científicas, Universidade Estadual de Santa Cruz, Rodovia Jorge Amado, 45662-900, Ilhéus, Bahia, Brazil

[69] Programa de Pós-graduação em Bioinformática, Universidade Federal de Minas Gerais, Av. Antônio Carlos, 31270-901, Pampulha, Belo Horizonte, MG, Brazil

[70] Biology Department & Ecology Program, The Pennsylvania State University, University Park, Pennsylvania, USA - 16802

[71] Forestry School, INDEHESA, Universidad de Extremadura, Plasencia, Spain

[72] U.S. Geological Survey, Southwest Biological Science Center, Flagstaff, AZ 86001 USA

[73] Cátedra de Ecología, Facultad de Agronomía, Universidad de Buenos Aires. Instituto de Investigaciones Fisiológicas y Ecológicas Vinculadas a la Agricultura (IFEVA-CONICET); Ciudad Autónoma de Buenos Aires, Argentina

[74] Universidad Nacional de Río Negro, Sede Atlántica, CEANPa; Río Negro, Argentina

[75] Cátedra de Manejo de Pastizales Naturales, Facultad de Ciencias Agrarias, Universidad Nacional de Catamarca, Catamarca, Argentina

[76] Universidad Estatal Amazónica (UEA), Puyo-Ecuador

[77] US Geological Survey, Southwest Biological Science Center; Moab, UT, USA

[78] Instituto Interuniversitario de Investigación del Sistema Tierra de Andalucía. Universidad de Jaén

[79] Institute of Ecology A.C. Environment and Sustainability Network, Chihuahua

[80] Global Drylands Center,School of Life Sciences and School of Sustainability,Arizona State University

[81] Al Quds University; Palestine

[82] Mara Research Station, Limpopo Department of Agriculture and Rural Development, South Africa

[83] Dead Sea and Arava Science Center, Yotvata, Israel

[84] Department of Geography and Earth Sciences, Aberystwyth University, Wales, UK

[85] School of Earth and Space Exploration, Arizona State University, Tempe, AZ, USA

[86] School of Life Sciences, Arizona State University, Tempe, AZ, USA

[87] Department of Planning and Environment, c/o Centre for Ecosystem Science, School of Biological, Earth and Environmental Sciences, University of New South Wales; Sydney, Australia

[88] Zoology Department, National Museums of Kenya, P.O. Box 40658-00100; Nairobi, Kenya

[89] Department of Earth and Environmental Sciences, Indiana University Indianapolis (IUI), Indianapolis, Indiana 46202, USA

[90] Key Laboratory of Vegetation Ecology of the Ministry of Education, Jilin Songnen Grassland Ecosystem National Observation and Research Station, Institute of Grassland Science, Northeast Normal University; Changchun, China

[91] Desert Ecology Research Group, School of Life and Environmental Sciences, The University of Sydney, Sydney, New South Wales 2006, Australia

[92] Forest and Rangeland Research Department, Khorasan Razavi Agricultural and Natural Resources Research and Education Center. AREEO, Mashhad, Iran.

[93] Department of Natural Resources, Agricultural Research Organization, Institute of Plant Sciences, Gilat Research Center; Mobile Post Negev, Israel

[94] State Key Laboratory of Desert and Oasis Ecology, Key Laboratory of Ecological Safety and Sustainable Development in Arid Lands, Xinjiang Institute of Ecology and Geography, Chinese Academy of Sciences

[95] Aix Marseille Univ, CNRS, Avignon Université, IRD, IMBE; Aix-en-Provence, France

Earth harbors an extraordinary plant phenotypic diversity[1] that is at risk from ongoing global changes[2,3]. However, we do not know how increasing aridity and livestock grazing pressure - two major global change drivers[4–6] shape the trait covariation underlying plant phenotypic diversity[1,7]. Here, we assessed how covariation among 20 chemical and morphological traits responds to aridity and grazing pressure within global drylands. Our analysis involved 133,769 trait measurements spanning 1,347 observations of 301 perennial plant species surveyed across 326 plots from six continents. Crossing an aridity threshold of ~0.7 (close to the transition between semi-arid and arid zones) led to an unexpected 88% increase in trait diversity. This threshold appeared in the presence of grazers, and moved toward lower aridity levels with increasing grazing pressure. Moreover, 57% of observed trait diversity only occurred in the most arid and grazed drylands, highlighting the phenotypic uniqueness of these extreme environments. Our work indicates that drylands act as a global reservoir of plant phenotypic diversity and challenge the pervasive view that harsh environmental conditions reduce plant trait diversity[8–10]. They also highlight that many alternative strategies may allow plants to cope with increases in environmental stress induced by climate change and land-use intensification.

The recent development of global trait databases[11] has been instrumental for characterizing the phenotypic diversity (trait diversity hereafter) of the entire plant kingdom[1,7,12]. This characterization is fundamental to anticipate the effects of global change on biodiversity and the functioning of the biosphere[2,13]. Yet, our understanding of plant trait diversity has been biased towards mesic biomes[14,15] (e.g., temperate regions). Although the geographical coverage of trait observations is currently increasing[11], many regions of the globe remain poorly explored[14,15]. In particular, drylands remain largely underrepresented in global trait databases[15] (Supplementary Table 1) despite the fact that they cover ~45% of the planet's terrestrial area[16], are present over all latitudes and continents[17], and are projected to expand due to climate change and associated increases in aridity[18] (defined as 1 - aridity index[5]; aridity index = mean annual precipitation ÷ potential evapotranspiration[19]). Drylands are highly vulnerable to multiple global change drivers[4–6] including changes in aridity and pressure from livestock grazing, the major land use across drylands[6]. For instance, crossing an aridity threshold of 0.7 or increasing grazing pressure can lead to abrupt and systemic changes in multiple ecosystem attributes[5,6], including drastic decreases in plant species richness and cover that may lead to land degradation

and desertification[20]. However, it remains virtually unknown how increasing aridity and grazing pressure jointly shape trait diversity of drylands at a global scale. This knowledge is needed to make reliable predictions of the future of biodiversity[2,13] and the functioning of dryland ecosystems[17,21] under global change.

One may expect that crossing aridity thresholds and increasing grazing pressure should reduce trait diversity in drylands[22] by selecting only those species able to tolerate extreme temperatures, low soil nutrient contents and water availability, and high stocking rates (see the pervasive "environmental filtering" concept[8–10] and associated hypotheses in Supplementary Text 1 and Supplementary Figure 1). However, drylands can exhibit a startling diversity of plant forms and functions[22,23] (the so-called "functional paradox of drylands"[17]), which seemingly contradicts the environmental filtering concept. This paradox may arise because distinct trait syndromes can perform equally in response to a specific environmental constraint[24,25], thus allowing alternative plant strategies to persist in harsh environments (Supplementary Text 1). Given the importance of trait diversity in the provisioning of essential ecosystem services[26] to the more than 2 billion people inhabiting dryland areas[20], understanding this discrepancy is a crucial research need.

Plant traits covary predictably among species because of evolutionary and ecological constraints limiting the number of viable trait combinations[1,7,12] that ultimately determine the extent of plant trait diversity[1]. Global initiatives aiming to characterize the fundamental dimensions of trait covariation have focused mainly on plant morphological diversity[1,7,12] and leaf carbon economy[27], but have largely neglected the diversity of chemical elements that sustain plant survival and growth[28,29]. The elemental concentration in plant leaves (plant elementome hereafter) has major implications for plant development[30], animal and human health[31,32], and global biogeochemical cycles[28]. Furthermore, the plant elementome has a pivotal role in determining plant responses to water scarcity[33–35] and herbivory[36,37] (Supplementary Table 2). However, we do not know how the plant elementome is distributed across plant species, and how it contributes to trait diversity patterns across global drylands. Accounting for the plant elementome may thus reveal new functional dimensions with the potential to change our understanding of plant strategies in drylands and their responses to ongoing global changes.

Here, we conducted a standardized field survey to investigate the impacts of aridity and grazing pressure on the chemical and morphological trait diversity of perennial plants across drylands worldwide (Figure 1). We selected 98 sites from 25 countries that represent the aridity

gradient over which dryland rangelands can be found globally[6]. Each site included three to four 45 m × 45 m plots spanning local gradients of grazing pressure (from ungrazed or low grazing pressure to high grazing pressure), with a total of 326 plots surveyed. In each plot, we measured a total of 20 continuous traits related to: i) the concentration of 14 chemical elements in plant leaves (i.e., C, N, P, K, Mg, Ca, S, Zn, Na, Cu, Mn, Fe, Ba, and Al), ii) the leaf and whole plant size (i.e., lateral spread, maximum plant height, leaf length, and leaf area), and iii) the leaf C-economy (i.e., specific leaf area, SLA; and leaf dry matter content, LDMC). Our study included 1,347 observations of 301 dryland plant species sampled across 326 plots from all latitudes and continents (Figure 1) for which the complete set of these 20 traits was measured (total number of traits measurements = 133,769; see Supplementary Table 3 for a full description of the data and Supplementary Figures 2-4 for the frequency distribution of these traits). This data constitutes a unique source of functional information to explore how aridity and grazing shape the covariations and trade-offs observed among multiple morphological and chemical plant traits across global drylands.

Trait diversity explodes in arid rangelands

We used a sliding windows analysis (see Methods) to evaluate changes in dryland trait diversity in response to increases in aridity and grazing pressure. To do so, we ordered the 326 plots surveyed according to their aridity level. We then defined aridity windows that represent 19% of the global aridity gradient considered, and selected all plant species from all plots within this aridity range (n = 307 observations in each window). For each aridity window, we quantified the *n*-dimensional trait space using the plant elementome, and morphological and C-economy related traits (i.e., trait hypervolume[38]; see Methods and Extended Data Figure 1, Supplementary Figures 5-8, and Supplementary Table 4 for a description of the dryland trait space evaluated). The size of the hypervolume provides a measure of the trait diversity[38] considered within each aridity window.

Increases in aridity were associated with an unforeseen increase in plant trait diversity (dashed line in Fig. 2a; see also Supplementary Table 5). We found a significant threshold response in the trait hypervolume occurring at an aridity value ~0.7 (Fig. 2). Aridity values exceeding this threshold were associated with an 88.1 % increase in the size of the trait hypervolume in the driest rangelands surveyed (Fig. 2b; Supplementary Figure 9). The trait hypervolume observed at high aridity levels largely encompassed and surpassed the

morphological and chemical trait diversity observed under low aridity conditions: 80.1 % of the low-aridity hypervolume was included within the high-aridity hypervolume and 57.3 % of the global dryland trait diversity was only observed under aridity values higher than ~0.7 (Fig. 2b). We also observed an increase of the size of the trait hypervolume with increasing grazing pressure (Fig. 2c). Aridity and grazing thus have a similar effect on trait diversity by promoting a wide spectrum of plant strategies to cope with water shortage[17,23,25] and herbivory[39,40] through a variety of avoidance and tolerance strategies. Our results support theoretical predictions[24] and empirical observations from drylands[17,22,23] and other extreme environments (e.g., alpine ecosystems[41]), which suggest that there are many ways for species to cope with climatic extremes and grazing pressure. The most arid dryland rangelands thus harbor a unique trait diversity, highlighting their importance as a global reservoir of plant form and function and reinforcing the biological and evolutionary importance of dryland ecosystems.

The elementome responds to global change

The sharp increase in trait diversity observed with increases in aridity and grazing pressure resulted mainly from a decrease in trait covariation at aridity values higher than ~0.7 (Fig. 3). Specifically, both aridity (Extended Data Figure 2; Supplementary Table 4) and the presence of grazers (Extended Data Figure 3; Supplementary Table 6) increased the number of trait dimensions within the dryland plant trait spectrum, resulting in the presence of extreme phenotypes exhibiting unique trait syndromes in the driest rangelands surveyed. For instance, all macronutrients correlated along a unique principal component (PC) axis below the ~0.7 aridity threshold (PC1 in Extended Data Figure 2a, b). After exceeding the ~0.7 aridity threshold, primary and secondary macronutrients - namely N-P-K and Mg-Ca-S - became independent and segregated along two different axes (Extended Data Figure 2c, d, e), highlighting a decoupling between macronutrients in plants under high aridity conditions.

High aridity levels also promoted functionally contrasting strategies (see Extended Data Figure 4), such as tall species with fast growing leaves following stress-avoidance strategies[22,25] (defined by high N-P-K and low LDMC values) and small conservative species following stress-tolerance strategies[1,42] (defined by low N-P-K and high LDMC values; Extended Data Figure 4b) with either low or high Mg-Ca (Extended Data Figure 4a), and Zn-Na (Extended Data Figure 4c) concentrations in leaves. These elemental strategies can reflect the contrasting role of chemical elements in plants, either as a way to tolerate high aridity levels[33–35], or as base

elements for defensive compounds against herbivory[36,37,43] (Supplementary Table 2). By identifying an abrupt change in trait variations among plant chemical elements occurring at aridity values ~0.7, our findings highlight the importance of considering the plant elementome to accurately grasp dryland biodiversity responses to ongoing climate change.

Resolving the dryland functional paradox

The abrupt increase in trait diversity with aridity observed corresponds with one of the recently identified ecosystem thresholds operating on drylands worldwide[5], which is characterized by declines in soil fertility and plant cover after an aridity value of ~0.7 is crossed. The simultaneous occurrence of alterations in crucial aspects of drylands and trait diversity presents a distinctive opportunity to uncover the underlying mechanisms through which increasing aridity and grazing pressure impact on dryland ecosystems.

We first hypothesized that abrupt declines in soil fertility could explain the changes in plant trait diversity observed once the aridity threshold of ~0.7 is crossed. This is attributed to the fact that variations in the chemical diversity of soils (the soil elementome) across different sites can directly affect the plant elementome[29,44]. We tested this hypothesis by measuring the soil elemental concentration of the 326 plots surveyed (see Methods; and Extended Data Figure 5). Contrary to what is observed across plant leaves (Extended Data Figure 1; Supplementary Figure 5), we found a strong covariation within the soil elementome (Extended Data Figure 5a, b; Supplementary Figure 10). All soil elements aligned along a unique principal component that accounts for 65.8% of the total variation observed in the soil elementome, a pattern that further increased in the most arid areas (Extended Data Figure 5c; Supplementary Table 7). These results did not support our hypothesis. Rather, they suggest a strong decoupling between the soil and plant elementome, and therefore that plant elemental concentration reflects independent dimensions through which dryland plant species segregate across contrasting functional strategies[29].

Alternatively, we hypothesized that declines in plant cover may explain the observed pattern of increased trait diversity with aridity. Since the decline in plant cover can alter interactions among plants (e.g., release of competitive interactions and collapse of positive interactions – incl. facilitation and plant-soil feedback[5,42,45]), we expected that increasing aridity would promote the persistence of competitively weak, but well-adapted phenotypes to aridity (see Supplementary Text 2 and Supplementary Figures 11, 12 for a rationale for this

hypothesis). To test this hypothesis, we measured *in situ* total plant cover across all of our sites (see Methods) and found that it was sharply reduced below ~ 50% after crossing the ~0.7 aridity threshold (Extended Data Figure 6). We substituted aridity with plant cover in our sliding windows procedure, and showed that crossing a ~ 50% value in plant cover was associated with both an increase in the trait hypervolume and a decrease in trait covariation (Extended Data Figure 7; Supplementary Table 8). At cover values higher than 50%, large vegetation patches may emerge from spatial constraints only (see the so-called spanning clusters in percolation theory[46–48]) forcing plant individuals to compete for space. In contrast, the decrease in plant cover below 50% may release competitive interactions as plant individuals would have space to thrive by avoiding competitive interactions[42,45]. The match between the ~0.7 aridity threshold and the 50% threshold in plant cover therefore reinforces our hypothesis that the observed pattern of increase in trait diversity with aridity may be driven by a collapse of plant-plant interactions[5,45]. Our results challenge the pervasive environmental filtering concept[8–10], which posits that the abiotic environment should select for a narrow set of trait values and reduce trait diversity in the most severe environments. In contrast, they revealed that increasing plant cover and the associated biotic processes[42,45] act as a global filter of plant biodiversity thereby reducing plant phenotypic diversity by half in the most productive compared to the most arid dryland areas.

Grazing was a main driver of decreasing plant cover (Extended Data Figure 6a, c) and significantly modulated both the shape and location of the aridity threshold (Fig. 4; and Supplementary Table 9), indicating that climate and land use changes interact to determine phenotypic plant diversity. Specifically, the absence of grazing shifted the observed aridity threshold for trait covariation towards a higher aridity value compared to other grazing pressure levels (Fig. 4). Furthermore, removing grazing smoothed aridity impacts on trait hypervolume, leading to a weak linear response of trait diversity to aridity observed in absence of grazers (Fig. 4). Altogether, our results also show that by modifying plant cover, grazing pressure can modulate the response of trait diversity to increasing aridity, and thus alter the trait space of dryland plant species worldwide.

Our results shed new light on the dryland functional paradox[17] by identifying a "plant loneliness syndrome", where the scattered plants across the most arid rangeland landscapes in drylands exhibit high degree of trait uniqueness. This syndrome may directly result from the collapse of biotic interactions associated with the low plant cover occurring in these environments[45,48], and from the large spatio-temporal variation in the distribution of limiting

resources[49]. Regardless of the mechanisms involved, the "plant loneliness syndrome" promotes a strikingly high plant trait diversity at the dry edge of perennial plant life. Combined with the general decline in plant taxonomic richness observed in the most arid drylands[5], our results highlight a very low functional redundancy in the species pool of the dryland plant flora, which could compromise their resistance and resilience to further disturbances[50].

Conclusion

We identified an abrupt reorganization of the dryland trait space after crossing an aridity value of ~0.7. Once this threshold was reached, small increases in aridity led to an abrupt increase of trait diversity. These changes were linked to a decoupling in the plant elementome. Similarly, increases in grazing pressure substantially increased trait diversity and modulated the aridity threshold identified. Our findings illustrate how climate and land use interact to shape phenotypic plant diversity in drylands, and bring both empirical and mechanistic evidence to the "dryland functional paradox"[17]. They question the predictions of the pervasive environmental filtering concept[8–10] that single trait optima allow species to persist in new environments. Our study also delivers novel insights into how vascular plants respond to biotic stressors and environmental extremes, and shed light on how the global plant functional trait space may be shaped by joint increases in aridity and grazing pressure, which are becoming more common in a drier and human-dominated world. Finally, our results can help to better understand the provisioning of essential nutrients to livestock and human populations in drylands under ongoing global environmental change.

References (Main Text)

1. Díaz, S. *et al.* The global spectrum of plant form and function. *Nature* **529**, 167–171 (2016).
2. IPBES. *Summary for Policymakers of the Global Assessment Report on Biodiversity and Ecosystem Services*. (2019) doi:10.5281/zenodo.3553579.
3. Carmona, C. P. *et al.* Erosion of global functional diversity across the tree of life. *Sci. Adv.* **7**, eabf2675 (2021).
4. Shukla, P. R. *et al.* Climate Change and Land: an IPCC special report on climate change, desertification, land degradation, sustainable land management, food security, and greenhouse gas fluxes in terrestrial ecosystems. (2019).
5. Berdugo, M. *et al.* Global ecosystem thresholds driven by aridity. *Science* **367**, 787–790 (2020).
6. Maestre, F. T. *et al.* Grazing and ecosystem service delivery in global drylands. *Science* **378**, 915–920 (2022).
7. Joswig, J. S. *et al.* Climatic and soil factors explain the two-dimensional spectrum of global plant trait variation. *Nature Ecology & Evolution* **6**, 36–50 (2022).
8. Keddy, P. A. Assembly and response rules: two goals for predictive community ecology. *J Vegetation Science* **3**, 157–164 (1992).
9. Kraft, N. J. B. *et al.* Community assembly, coexistence and the environmental filtering metaphor. *Functional Ecology* **29**, 592–599 (2015).
10. Enquist, B. J. *et al.* Scaling from traits to ecosystems: developing a general trait driver theory via integrating trait-based and metabolic scaling theories. in *Advances in ecological research* vol. 52 249–318 (Elsevier, 2015).
11. Kattge, J. *et al.* TRY plant trait database – enhanced coverage and open access. *Global Change Biology* **26**, 119–188 (2020).
12. Carmona, C. P. *et al.* Fine-root traits in the global spectrum of plant form and function. *Nature* **597**, 683–687 (2021).
13. Urban, M. C. *et al.* Improving the forecast for biodiversity under climate change. *Science* **353**, aad8466 (2016).
14. Maitner, B. *et al.* A global assessment of the Raunkiæran shortfall in plants: geographic biases in our knowledge of plant traits. *New Phytologist* **240**, 1345–1354 (2023).

15. Thomas, H. J. *et al.* Global plant trait relationships extend to the climatic extremes of the tundra biome. *Nature communications* **11**, 1351 (2020).

16. Prăvălie, R. Drylands extent and environmental issues. A global approach. *Earth-Science Reviews* **161**, 259–278 (2016).

17. Maestre, F. T. *et al.* Biogeography of global drylands. *New Phytologist* **231**, 540–558 (2021).

18. Chai, R. *et al.* Human-caused long-term changes in global aridity. *npj Climate and Atmospheric Science* **4**, 65 (2021).

19. Lian, X. *et al.* Multifaceted characteristics of dryland aridity changes in a warming world. *Nature Reviews Earth & Environment* **2**, 232–250 (2021).

20. Reynolds, J. F. Desertification. in *Encyclopedia of Biodiversity* (ed. Levin, S. A.) 61–78 (Elsevier, New York, 2001).

21. Van Bodegom, P. M., Douma, J. C. & Verheijen, L. M. A fully traits-based approach to modeling global vegetation distribution. *Proc. Natl. Acad. Sci. U.S.A.* **111**, 13733–13738 (2014).

22. Le Bagousse-Pinguet, Y. *et al.* Testing the environmental filtering concept in global drylands. *Journal of Ecology* **105**, 1058–1069 (2017).

23. Noy-Meir, I. Desert Ecosystems: Environment and Producers. *Annu. Rev. Ecol. Syst.* **4**, 25–51 (1973).

24. Marks, C. O. & Lechowicz, M. J. Alternative Designs and the Evolution of Functional Diversity. *The American Naturalist* **167**, 55–66 (2006).

25. Volaire, F. A unified framework of plant adaptive strategies to drought: Crossing scales and disciplines. *Global Change Biology* **24**, 2929–2938 (2018).

26. Gross, N. *et al.* Functional trait diversity maximizes ecosystem multifunctionality. *Nature ecology & evolution* **1**, 0132 (2017).

27. Wright, I. J. *et al.* The worldwide leaf economics spectrum. *Nature* **428**, 821–827 (2004).

28. Fernández-Martínez, M. From atoms to ecosystems: elementome diversity meets ecosystem functioning. *New Phytologist* **234**, 35–42 (2022).

29. Peñuelas, J. *et al.* The bioelements, the elementome, and the biogeochemical niche. *Ecology* **100**, e02652 (2019).

30. Baxter, I. & Dilkes, B. P. Elemental Profiles Reflect Plant Adaptations to the Environment. *Science* **336**, 1661–1663 (2012).

31. White, P. J. & Brown, P. Plant nutrition for sustainable development and global health. *Annals of botany* **105**, 1073–1080 (2010).

32. Kaspari, M., De Beurs, K. M. & Welti, E. A. R. How and why plant ionomes vary across North American grasslands and its implications for herbivore abundance. *Ecology* **102**, e03459 (2021).

33. Lanning, M. *et al.* Intensified vegetation water use under acid deposition. *Sci. Adv.* **5**, eaav5168 (2019).

34. Golldack, D., Li, C., Mohan, H. & Probst, N. Tolerance to drought and salt stress in plants: unraveling the signaling networks. *Frontiers in plant science* **5**, 151 (2014).

35. Morales, F., Pavlovič, A., Abadía, A. & Abadía, J. Photosynthesis in Poor Nutrient Soils, in Compacted Soils, and under Drought. in *The Leaf: A Platform for Performing Photosynthesis* (eds. Adams Iii, W. W. & Terashima, I.) vol. 44 371–399 (Springer International Publishing, Cham, 2018).

36. Mládková, P., Mládek, J., Hejduk, S., Hejcman, M. & Pakeman, R. J. Calcium plus magnesium indicates digestibility: the significance of the second major axis of plant chemical variation for ecological processes. *Ecology Letters* **21**, 885–895 (2018).

37. Boyd, R. Elemental defenses of plants by metals. *Nature Education Knowledge* **1**, (2010).

38. Blonder, B., Lamanna, C., Violle, C. & Enquist, B. J. The *n* -dimensional hypervolume. *Global Ecology and Biogeography* **23**, 595–609 (2014).

39. Moles, A. T. *et al.* Correlations between physical and chemical defences in plants: tradeoffs, syndromes, or just many different ways to skin a herbivorous cat? *New Phytologist* **198**, 252–263 (2013).

40. Briske, D. D. Strategies of plant survival in grazed systems: a functional interpretation. *The ecology and management of grazing systems* 37–67 (1996).

41. Körner, C. *Alpine Plant Life*. (Springer Berlin Heidelberg, Berlin, Heidelberg, 2003). doi:10.1007/978-3-642-18970-8.

42. Grime, J. P. Evidence for the Existence of Three Primary Strategies in Plants and Its Relevance to Ecological and Evolutionary Theory. *The American Naturalist* **111**, 1169–1194 (1977).

43. He, H., Bleby, T. M., Veneklaas, E. J., Lambers, H. & Kuo, J. Precipitation of calcium, magnesium, strontium and barium in tissues of four Acacia species (Leguminosae: Mimosoideae). *PLoS one* **7**, e41563 (2012).

44. Han, W. X., Fang, J. Y., Reich, P. B., Ian Woodward, F. & Wang, Z. H. Biogeography and variability of eleven mineral elements in plant leaves across gradients of climate, soil and plant functional type in China: Biogeography and variability of leaf chemistry. *Ecology Letters* **14**, 788–796 (2011).

45. Michalet, R., Le Bagousse-Pinguet, Y., Maalouf, J. & Lortie, C. J. Two alternatives to the stress-gradient hypothesis at the edge of life: the collapse of facilitation and the switch from facilitation to competition. *J Vegetation Science* **25**, 609–613 (2014).

46. Rietkerk, M. & van de Koppel, J. Alternate stable states and threshold effects in semi-arid grazing systems. *Oikos* 69–76 (1997).

47. Abades, S. R., Gaxiola, A. & Marquet, P. A. Fire, percolation thresholds and the savanna forest transition: a neutral model approach. *Journal of Ecology* **102**, 1386–1393 (2014).

48. Berdugo, M. *et al.* Aridity preferences alter the relative importance of abiotic and biotic drivers on plant species abundance in global drylands. *Journal of Ecology* **107**, 190–202 (2019).

49. Chesson, P. Mechanisms of Maintenance of Species Diversity. *Annu. Rev. Ecol. Syst.* **31**, 343–366 (2000).

50. Biggs, C. R. *et al.* Does functional redundancy affect ecological stability and resilience? A review and meta-analysis. *Ecosphere* **11**, e03184 (2020).

Figure Captions

Fig. 1: A survey of plant trait diversity across global dryland rangelands. The data included 1,347 observations of 301 perennial plant species, which provided a complete set of measurements for the 20 traits (see Supplementary Table 3 for details). The color of the dots represented the aridity level of each of the 98 dryland sites where plant traits have been measured. Each site included three to four plots locally distributed along a grazing gradient (326 plots surveyed in total, see Methods). The size of the dots indicated the number of species sampled in each plot (mean number per plot = 4.6 species; minimum number per plot = 1 species; Maximum number per plot 18 species). The selected sites were globally distributed across all latitudes and continents (except Antarctica), and are representative of the wide variation in climates, soil properties, and vegetation types found across global drylands[6,17]. Aridity = 1 - Aridity index (precipitation/potential evapotranspiration).

Fig. 2: Global increase in dryland plant trait diversity driven by aridity and grazing. a shows aridity effect on the size of the trait hypervolume. We found a significant, non-linear increase in the hypervolume size once an aridity threshold ~0.7 was crossed. Vertical dashed and dotted lines represent the mean location of the threshold and 0.95 confidence interval, respectively (Supplementary Table 5). Colored dots represent bootstrapped values for trait hypervolume. Error band shows the 95 % confidence interval. **b** shows the bootstrapped values for the hypervolume size below and above this aridity threshold (low aridity n = 189; high aridity n = 696). After crossing the ~0.7 aridity threshold, the hypervolume increased by 88.1 % because it included not only most of the trait variability observed under low aridity conditions (only 19.9 % of uniqueness), but also 57.3% of trait diversity that only occurs in the most arid conditions. **c** shows the bootstrapped values for trait hypervolume for each grazing pressure level (High Grazing n = 382; Medium Grazing n = 410; Low Grazing n = 389; Ungrazed n = 166). Bootstrapped values were generated using a random sampling of n = 100 observations for 100 times in each aridity and grazing level. In **b-c** data are represented as boxplots where the middle line is the median, the lower and upper hinges correspond to the first and third quartiles, the upper and lower lines show the 0.95 confidence intervals. In **b-c**, we tested whether different aridity and grazing pressure levels showed significant differences using a generalized least squares model ($p < 0.001$ for both aridity in **b** and grazing in **c**). In **c**, letters show results of a post-hoc test based on bootstrapped pairwise comparisons between grazing pressure levels. Different letters indicate significant differences among grazing pressure levels.

570 Fig. 3: **Abrupt changes in trait covariations after crossing the ~0.7 aridity threshold. a**
571 shows how the strength of trait covariations, measured using a phenotypic integration index
572 (see Methods), decreased with aridity. We found a significant, non-linear decline at aridity
573 values ~ 0.7 (see Supplementary Table 5 for more detailed results). Vertical dashed and dotted
574 lines represent the mean location of the threshold and its 0.95 confidence interval, respectively.
575 Colored dots represent bootstrapped values for trait covariation for each aridity level. Error
576 band shows the 95 % confidence interval. **b** shows the bootstrapped values for trait covariation
577 for each grazing pressure level (High Grazing n = 382; Medium Grazing n = 410; Low Grazing
578 n = 389; Ungrazed n = 166). Bootstrapped values were generated using a random sampling of
579 n = 100 observations for 100 times in each aridity and grazing level. In **b** data are represented
580 as boxplots where the middle line is the median, the lower and upper hinges correspond to the
581 first and third quartiles, the upper and lower lines show the 0.95 confidence interval. Data
582 beyond the confidence interval are outlying points that are plotted individually. In **b**, we tested
583 whether different grazing pressure levels showed significant differences using a generalized
584 least squares model ($p < 0.001$). Letters show results of a post-hoc test based on bootstrapped
585 pairwise comparisons between grazing pressure levels. Different letters indicate significant
586 differences among grazing pressure levels.

587

588 Fig. 4: **Interactions between grazing and aridity drive trait covariation and diversity**
589 **across global drylands. a-b** show how grazing modulates the hypervolume size and trait
590 covariation in response to aridity (High Grazing n = 382; Medium Grazing n = 410; Low
591 Grazing n = 389; Ungrazed n = 166). Error band shows the 0.95 confidence interval. Colored
592 dots represent bootstrapped values for trait hypervolume for each aridity level. Grazing both
593 changed the shape of the aridity response (see Supplementary Table 9 for model selection for
594 each grazing level) and the location of the threshold (vertical colored dashed lines). **c-d** show
595 the bootstrapped location of the aridity-threshold at each grazing level using boxplots where
596 the middle line is the median, the lower and upper hinges correspond to the first and third
597 quartiles, the upper and lower lines show the 0.95 confidence interval. Data beyond the
598 confidence interval are outlying points that are plotted individually. In **c-d**, we tested whether
599 different grazing pressure levels showed significant differences using a generalized least
600 squares model ($p < 0.001$). Letters show results of a post-hoc test based on bootstrapped
601 pairwise comparisons between grazing pressure levels. Different letters indicate significant
602 differences among grazing pressure levels. We found significant threshold-responses were

observed under grazing (low, medium and high grazing pressures) on trait hypervolume (**a**-**c**) while trait hypervolume remained constantly low as aridity increased and increased linearly when grazing was removed (ungrazed plots). For trait covariation (**b**-**d**), the thresholds appeared at lower aridity levels under increasing grazing pressure.

Methods

Further details on methods are given in the Supplementary Information.

Study site selection

Our study focused on drylands, areas where rainfall is < 65% of the evaporative demand[51]. We surveyed 98 dryland sites located in 25 countries from six continents (Algeria, Argentina, Australia, Botswana, Brazil, Canada, Chile, China, Ecuador, Hungary, Iran, Israel, Kazakhstan, Kenya, Mexico, Mongolia, Namibia, Niger, Palestine, Peru, Portugal, South Africa, Spain, Tunisia, and the United States of America) (Figure 1). Site selection captured most of the aridity conditions, vegetation (shrublands, grasslands, open woodlands, savannahs, and steppes) and soil types that can be found in drylands worldwide (see refs.[6,52] for more detailed explanation on site selection). At each of the 98 study sites surveyed, three to four 45 m × 45 m plots (total N = 326 plots) were selected along a local grazing gradient (ungrazed, low, medium, and high grazing pressure), which was largely driven by livestock (but also included native herbivores[6]). Each grazing gradient was established using the distance to artificial water points and grazing exclosures when available (see ref.[6] for a detailed assessment of the validation of the local grazing gradients surveyed). In our dataset, aridity was defined as 1 - aridity index (AI, mean annual precipitation/potential evapotranspiration[51]) following ref.[5]. Aridity ranged between 0.48 (wettest) to 0.99 (driest) across the surveyed drylands. This aridity range corresponds to a gradient of mean annual precipitation between 891 and 29 mm/yr, and to a gradient of mean annual temperature between -1.2 and 29.2°C. Our survey also captured most of the variation in grazing pressure that can be found across dryland rangelands worldwide[6].

Plant trait sampling

Fieldwork was conducted between January 2016 and September 2019. Vegetation surveys were carried out after the main rainfall season at each site to ensure surveying during (or just after) the main peak biomass. This approach allowed us to standardize the sampling while accounting for differences in vegetation phenology among contrasted biogeographical regions, continents, and hemispheres. We restricted our study to perennial plants because they represent 94% of the plant species on earth[53] and are instrumental in maintaining the functioning of drylands[26,54–56].

We focused on 20 continuous traits related to the morphological and chemical diversity of plants, which were measured following the most updated standardized protocols[57,58]. These traits included: i) whole-plant and leaf size related traits[1,59] (maximum plant height [H, cm], plant lateral spread [LS, cm^2], leaf length [LL, cm] and leaf area [LA, cm^2]); ii) leaf traits related to carbon-economy and herbivory[27,32,40,60,61] (Specific leaf area [SLA, $cm^2.g^{-1}$], leaf dry matter content [LDMC, $g.g^{-1}$]); and iii) the foliar concentration of 14 chemical elements that characterize the plant elementome[28,29,32,62] (C, N, P, K, Mg, Ca, Zn, S, Na, Cu, Fe, Al, Mn, and Ba). These traits were measured *in situ* within each of the 326 plots. To do so, four 45 m transects oriented downslope were established within each plot, and spaced 10 m apart. We then placed 25 contiguous quadrats (1.5 m × 1.5 m) along each transect (100 quadrats per plot). Trait measurements were performed on five quadrats randomly selected in each transect (i.e., five quadrats x four transects = 20 quadrats per plot). In each quadrat, we selected the most developed individual of each perennial species present. Our sampling protocol is highly suitable to account for both local trait abundances (because frequent species will have more samples than rare species[63,64]) and between-plot intraspecific trait variability[65]. See ref.[52] for a detailed description of the sampling protocol followed.

We measured plant height, i.e. the height of the selected individual from the ground to the highest leaves belonging to the vegetative part of the plant; and the lateral spread using two perpendicular measurements of plant width. On the same individual, we then sampled mature and undamaged leaves at the top of the plant to ensure a development under full-light conditions (sampled leaf surface was always > 2 cm^2). Leaves were stored in moistened plastic bags and brought to the laboratory for rehydration, before leaf area and leaf mass measurements.

We measured the leaf area of each sampled individual by taking pictures of the collected leaves flattened below a glass sheet, and analyzed them using the freeware ImageJ[66] (https://imagej.nih.gov/ij/index.html; see ref.[52] for additional details). Leaf fresh and dry mass for each sampled individual were obtained by weighing before and after oven drying at 60 ºC for 48 h. Then, dry leaves were grouped by species within each plot in paper bags and were shipped to the laboratory of Rey Juan Carlos University in Móstoles (Spain) for chemical analyses. These shipments were carried out according to national and international regulations; exporting permits were obtained for each country (when required) and importing permits to Spain were obtained for every shipment by the Spanish Ministry of Agriculture, Fisheries and Food.

669 Once in the laboratory, oven-dried leaves were ground in a homogenizer (Precellys®
670 24; Bertin Technologies, Montigny-le-Bretonneux, France) and analyzed for total nitrogen and
671 total carbon on a EuroEA3000 elemental analyser (EuroVector, Pavia, Italy). Total chemical
672 elements in leaves (P, K, Mg, Ca, Cu, Zn, S, Na, Fe, Al, Mn, and Ba) were analyzed by
673 inductively coupled plasma optical emission spectrometry with a Perkin Elmer Optima 4300
674 DV (Perkin Elmer, Waltham, Massachusetts, USA) after open-vessel nitric-perchloric acid wet
675 digestion. At the end of this procedure, we obtained the foliar concentration of the 14 elements
676 for each species sampled in each plot.

677

678 **Plant cover and soil properties measurements**

679 We quantified vegetation cover in each plot using the line-point intercept method[52]. We
680 recorded points located every 20 cm along each of the four transects for a total of 225 points
681 per transect (900 points per plot; see ref. 54 for additional details on this survey). Vegetation
682 cover was calculated as the proportion of points where perennial plants were recorded.

683 We also quantified the elemental concentrations of the soil beneath plant canopies in
684 each of the 326 plots surveyed in the peak of the dry season to ensure that the data obtained
685 across sites were as standardized and comparable as possible[6]. At each plot, five 50 cm × 50
686 cm quadrats were randomly placed under the canopy of the dominant (in terms of % cover)
687 perennial plant species. A composite topsoil sample consisting of five 145 cm^3 soil cores (0-
688 7.5 cm depth) was collected from each quadrat, bulked, and homogenized in the field (five
689 composite samples per plot were obtained). After field collection, the soil samples were taken
690 to the laboratory, where they were sieved (2 mm mesh). Once sieved, samples were air-dried
691 for one month and stored for physico-chemical analyses. Dried soil samples from all the
692 countries were shipped to the laboratory of Rey Juan Carlos University in Móstoles (Spain) for
693 analyses. Once in the laboratory, replicated soil samples were bulked to obtain a composite
694 sample per plot. Total C and N concentration in soils was determined on ball-milled soils by
695 dry combustion, gas chromatography and thermal conductivity detection, after removing
696 carbonates by acid fumigation. Total P, K, Mg, Ca, Cu, Zn, S, Na, Fe, Al, Mn, and Ba were
697 extracted by open-vessel nitric-perchloric acid wet digestion, re-suspended in water, and
698 measured by inductively coupled plasma optical emission spectrometry[67,68] (ICP-OES Perkin
699 Elmer Optima 4300 DV).

Soil pH was measured in all the soil samples with a pH meter, in a 1: 1 soil to water (w:v) suspension[52]. Soil texture (sand, clay, and silt content) was measured according to ref.[69]. The three textural variables measured (sand, clay, and silt) were highly intercorrelated (Spearman $\rho_{sand\text{-}silt}$ = -0.987, $P < 0.001$; Spearman $\rho_{sand\text{-}clay}$ = -0.851, $P < 0.001$; Spearman $\rho_{silt\text{-}clay}$ = 0.766, $P < 0.001$). Thus, we selected just one of these fractions (sand), to use in our data analyses because this fraction is less prone to measurement errors given the method used.

Data management and gap-filling procedure

We compiled a database of 133,769 trait measurements, where each species in each plot was tagged as a unique ID (Supplementary Table 3). Species taxonomy was standardized according to World of Flora (WFO (2023): World Flora Online. http://www.worldfloraonline.org). 99.5% of the individual plants were identified at the genus level, and 93.6% at the species level. We used pseudo-species names for the 6.4% of species (n = 18 species) that could not be identified. To ensure a high level of data quality, all trait measurements were inspected using a semi-automated procedure and corrected when possible following guidelines from ref.[11]. Specifically, we looked for potential systematic errors, including wrong units or the presence of aberrant traits values for each species and trait measured.

Morphological traits (H, LS, LL, LA, SLA, LDMC) were available at the individual level (20,961 individual plants measured). Traits related to leaf nutrients were available at the plot level for each species. To homogenize the level of analysis for all traits, we averaged individual morphological measurements to obtain a single trait value for each species in each of the 326 plots. For plant H and LS, we also recorded the maximum value observed in each plot and for each species to characterize plant species maximum H and LS following ref.[57].

Data completeness varied among traits (Supplementary Table 3) but overall offered a high degree of representativeness and geographical coverage at a global scale (Figure 1). We did not have missing data for morphological traits (H, LS, LL). The levels of data completeness for LA, SLA, LDMC were very high: 95%, 93%, and 89%, respectively. Missing data for these variables were mainly due to methodological reasons, such as the inability to ensure a proper leaf rehydration when measuring leaf fresh mass for LDMC. The amount of leaf dry material sampled in the field was lower than the minimum required for some analyses for rare species (for which the leaves of less than three individuals per plot were sampled). Thus, the number of trait samples also differed among leaf nutrients (CN *vs.* other macro- and microelements)

due to the amount of leaf dry material available for analyses (2 mg of dry mass for C/N analyses vs. 800 mg of dry mass for other elements). In total, the level of data completeness for chemical traits was > 70% for C and N concentration in leaves and > 50 % for other macro and microelements (Supplementary Table 3).

Data completeness is a fundamental prerequisite of trait covariation analyses because multivariate analyses require a full set of trait information for all species considered. Indeed, a missing value for one trait leads to systematic deletion of the whole species. Therefore, a gap-filling procedure in the data trait matrices is a suitable approach to reduce this problem[70–72]. Here, we used a highly conservative gap-filling procedure based on the following criteria: i) we used only trait data measured from our trait sampling, i.e. we did not retrieve trait data from external databases such as TRY[11]; ii) the gap-filling procedure was performed within species in all cases (i.e., only when trait values were available for the same species in another plot); and iii) we developed an algorithm to optimize the gap-filling procedure according to both aridity and grazing pressure levels instead of using phylogenetic relatedness[73]. Specifically, when a trait value is missing for a given species in a given plot, the algorithm allows filling the missing data by maximizing the match between the species trait value and the local environmental conditions (see all details of the gap-filling procedure in Supplementary Text 3; Supplementary Figures 13-15). Gap-filling significantly improved data representativeness by increasing the number of species considered (Supplementary Table 3) without biasing the trait database. Indeed, we observed remarkably low imputation errors (11 ± 8 %) for most chemical traits, indicating that within species trait variability of the plant elementome is negligible compared to what is observed across species (see additional results in Supplementary Text 3; Supplementary Figures 7-8).

At the end of the procedure, a total of 1,347 observations of 301 dryland plant species measured across the 326 plots with the complete set of traits were available for analyses (compared to 887 observations before gap-filling, see Supplementary Table 3; Supplementary Figure 16). The n = 1,347 observations were consistently used in all main analyses.

Statistics and Reproducibility

We conducted all statistical analyses using the statistical software R 4.3.2 (2023-10-31 ucrt).

Characterizing the dryland trait space

To quantify the trait diversity of dryland plant species, we first determined the fundamental trait dimensions along which dryland plant species segregate. To do this, we ran a series of principal component analyses (PCAs) using the complete set of measured traits (Extended Data Figure 1) and plant chemical elements only (Supplementary Figure 5). Traits were log-transformed and scaled before analysis[12] (see the distribution of each trait in Supplementary Figures 2-4). We used the Horn's parallel analysis from the R package *paran*[74] to determine the dimensionality of the PCAs[12], and applied a varimax rotation procedure to facilitate the interpretation of the results.

PCAs are standard tools in trait spectrum analyses[1,12,15,75]. They efficiently summarize the covariations and trade-offs observed among multiple traits by representing the trait loadings (arrows in Extended Data Figure 1) along the PCA axes (calculated from the eigenvectors of each trait and the eigenvalues of each axis). The % of variance explained by each selected axis represents the importance of each PCA dimension in explaining the observed trait variability across species. Eigenvalues were further used to calculate an index of phenotypic integration, which summarizes the strength of trait covariation[76–78]. This phenotypic integration index was calculated using the variance of the eigenvalues as:

$$Var(\gamma) = \sum_{i=1}^{N}(\gamma_i - 1)^2/N \qquad \text{equation 1}$$

where γ_i is the eigenvalue from the i-th dimension and N is the number of traits[79]. We used the eigenvalue of the un-rotated PCA to compute the phenotypic integration index. Higher values of this index indicate stronger covariations among N traits. When traits are uncorrelated, eigenvalues are similar and exhibit low variance. When traits are highly correlated, the first eigenvalue is much higher than the other eigenvalues, leading to high variance. PCA axes also provide information on the hypervolume[1,38,80,81] occupied by the studied species in a n-dimensional trait space, and thus the size of the hypervolume provides a measure of the trait diversity observed for a given species pool[80]. In this study, we used both hypervolumes and trait covariations to quantify the effects of aridity and grazing on the spectrum of plant traits observed in global drylands.

Evaluating the impacts of aridity on the dryland plant trait space

We used a sliding window analysis to evaluate how the hypervolume and trait covariation changed along the aridity gradient evaluated. This analysis is well suited to investigate how the correlation between different variables (here traits) change according to a third predictor (here aridity), and to evaluate whether these changes are linear or abrupt[48,82,83]. To do so, we first ordered the 326 plots surveyed according to their aridity level. We then selected all plots located within an aridity window of 0.1 (roughly equivalent to 19% of the total aridity gradient captured in our survey), starting from the lowest aridity value observed in our dataset. The width of the aridity window used was selected to ensure: i) enough statistical power (307 observations of dryland plant species on average within each window; with min = 103 and max = 473); ii) that the species pools selected in each window originated from plots characterized by different grazing pressure levels; and iii) that the selected species belonged to contrasted biogeographical regions across the world. Indeed, each aridity window included on average 19 sites (min = 8; max = 32) originated from different regions of the world to avoid spatial autocorrelation, see Figure 1). Therefore, our sliding windows analysis operates at a global scale to evaluate how global increases in aridity and grazing pressure influence the trait pool in drylands worldwide.

For each aridity window, we calculated the strength of trait covariations using the same PCA procedure as explained above and the diversity of trait values observed within this aridity range. We randomly sampled n = 100 observations within the window and extracted the eigenvalue of the significant selected axes, calculating their variance to obtain an index of phenotypic integration. We repeated the random sampling of n = 100 observations for 100 times within each window to calculate the confidence interval of the index for each aridity window. We used the same procedure to calculate the hypervolume using the R package *Hypervolume*[81]. To calculate the hypervolume, we used the PCA coordinates as trait values for the five dimensions of the dryland plant spectrum described in Extended Data Figure 4. We then moved the sliding window toward higher aridity levels of 0.01 by both adding the plots scoring the next aridity value and removing the plots with the lowest aridity. We repeated this analysis as many times as plots remained along the aridity gradient. We then plotted the results and tested how trait covariations in the dryland species pool and their diversity changed along the aridity gradient.

We evaluated whether the observed trait responses along the aridity gradient truly corresponded to an aridity-threshold by fitting threshold models using the R package *chngpt*[84]. In essence, these models find a breakpoint in the data by dividing it according to a predictor value (here aridity) and using two different fitting functions at each side of the breakpoint. To

assess whether these threshold models were a better fit to the data than a linear model we used the Bayesian information criterion (BIC), which measures the goodness of fit of the data based on log-likelihood of the fitting functions considering the number of parameters used[82]. The models exhibiting the lowest BIC values are the most parsimonious and provide the best fit. Differences in BIC <2 represent similarly good models[85]. Apart from a regular linear model, we used a generalized additive model and five different threshold models for extracting the BIC, each differing from each other by the functions fitted at both sides of the estimated breakpoint: step (two intercept models, for which the differences in intercept were tested at the breakpoint), segmented (two linear models in which the slope is changed at breakpoint), stegmented (two linear models in which both the slope and the intercept are changed at the breakpoint), hinge model 12 (one linear model is fitted for the left part of the breakpoint and a second degree polynomial is fitted for the right part), and hinge model 22 (two different second degree polynomial models are fitted at both sides of the breakpoint). The model (either linear or threshold-like) exhibiting the lowest BIC was considered the best model. Each of the threshold models considered allows the identification of a breakpoint with associated 0.95 confidence interval (CI) as a parameter resulting from the model fitting. We considered the aridity value at which a breakpoint was observed as the aridity threshold.

We observed non-linear, abrupt responses of trait covariations and hypervolumes at aridity ~0.7 based on the breakpoint analyses described above (Figs. 2 and 3). To further examine how aridity reshaped the dryland plant trait spectrum, we divided our data into two subsets: below and above aridity = 0.7 ± Confidence Interval (CI). We re-ran all the PCA analyses explained above to evaluate how aridity changed the dimensionality of the trait spectrum for these subsets of the data. We also re-calculated the hypervolume observed at low and high aridity values, and quantified their overlap using the function *hypervolume_overlap_statistics* in the R package *Hypervolume*[81]. This function provides the % of overlap between distinct hypervolumes, as well as the % of uniqueness of each hypervolume.

Assessing the impacts of grazing on the dryland plant trait space

To test for the effects of grazing pressure, we calculated the index of trait covariation and the hypervolumes for each grazing pressure level (ungrazed, low, medium, and high grazing pressure). We used a bootstrap procedure and repeated the calculation 100 times to obtain the confidence interval. We then tested whether different grazing pressure levels showed contrasted

values of these indices using a generalized least squares model to account for heteroscedasticity (using the function *gls* from the R package *nlme*[86]). To represent how different grazing pressures may alter the dryland plant trait space, we also re-ran the PCA analyses for each grazing pressure level evaluated (from ungrazed to high grazing pressure). Finally, we tested whether grazing pressure changed the shape and the location of the aridity threshold. To do so, we re-ran the sliding windows analysis conducted above, but at each grazing level separately. We tested whether grazing pressure (ungrazed, low, medium, and high grazing pressure) changed the location of the threshold. We extracted the bootstrap distribution of the threshold at each grazing pressure level, and tested, using generalized least square models, whether the location of the threshold was significantly shifted along the aridity gradient compared to the overall threshold found at aridity ~0.7.

Assessing the impacts of aridity and grazing on the soil elementome

We examined how chemical elements in soils (the soil elementome) responded to changes in aridity. We first conducted a PCA as explained above to evaluate how the concentrations of the 14 chemical elements in soils covary across the 326 sampled plots. We then extracted the PC coordinate of each selected axis and evaluated how the soil elementome responded to grazing and aridity using linear mixed effect models and the R package *lme4*[87]. We considered in the model the effect of grazing and aridity and used site as a random factor (random effect: 1|site), allowing model intercept to vary among sites since plots belonging to the same site correspond to a local grazing gradient that has been repeated across the 98 sites surveyed. Finally, we used the same sliding windows procedure as explained above to test how soil chemical diversity responded to aridity. All soil elements covaried along a unique PC axis accounting for 65.8% of the total variation (Extended Data Figure 5a, b). Because computing hypervolumes in one dimension is irrelevant[81], we therefore computed the sliding window analysis only to test whether covariation among multiple soil elements changed with increasing aridity (Extended Data Figure 5c).

Plant cover as a modulator of the effects of aridity and grazing on the dryland plant trait space

We evaluated how changes in plant cover observed across global drylands once the ~0.7 aridity threshold is crossed impacted on plant trait diversity. We first tested how aridity and grazing impacted plant cover using linear mixed effect models and the R package *lme4*[87]. Our model

included aridity, grazing, and an interaction between them. Site was used as a random factor (random effect: 1|site). The model also included a series of covariates known to impact plant cover[6] in drylands, such as latitude and longitude of our study sites, as well as their elevation and topography (slope and aspect). We used the sine and cosine of the longitude and aspect to avoid any bias due to intrinsic circularity of these predictors in the statistical models[22] (i.e., Longitude (sin) and Longitude (cos) hereafter, respectively). We also considered two soil master variables, i.e. sand content and soil pH[22,88]. A quadratic term was considered for pH. All predictors were scaled before analysis to facilitate the comparison of estimates.

The full model used was: lmer (Plant Cover ~ (1|site) + latitude + longitude (sin) + longitude (cos) + exposure (sin) + exposure (cos) + slope + elevation + aridity*grazing + sand + pH + pH^2). Using this full model, we ran a model averaging procedure to select the set of predictors that best explained variations in plant cover. To do this, we applied a multi-model inference procedure using the *MuMIn* R package[89]. This method allowed us to create a set of models with all possible combinations of the initial variables, which were fitted using a Maximum Likelihood procedure[90] and sorted according to the Akaike Information Criterion (AIC). Aridity and grazing were the main drivers of plant cover in our analyses (Extended Data Figure 6). Finally, we substituted aridity by plant cover in our sliding windows procedure to test how plant cover influenced hypervolume and trait covariation (Extended Data Figure 7).

Data availability

All processed datasets generated during the current study are available in the open source repository:

https://doi.org/10.57745/SFCXOO

Code availability

The R code used to analyze the data is available in the open source repository:

https://doi.org/10.57745/SFCXOO

References (Methods)

51. ILRI, I. UNEP and ILC. 2021. *Rangelands Atlas. Nairobi Kenya: ILRI For more information on the Atlas please contact: Fiona Flintan, Senior Scientist, ILRI f. flintan@ cgiar. org BY CC* 4 (2021).

52. Maestre, F. T. *et al.* The BIODESERT survey: Assessing the impacts of grazing on the structure and functioning of global drylands. *Web Ecology* **22**, 75–96 (2022).

53. Poppenwimer, T., Mayrose, I. & DeMalach, N. Revising the global biogeography of annual and perennial plants. *Nature* **624**, 109–114 (2023).

54. García-Palacios, P., Gross, N., Gaitán, J. & Maestre, F. T. Climate mediates the biodiversity–ecosystem stability relationship globally. *Proc. Natl. Acad. Sci. U.S.A.* **115**, 8400–8405 (2018).

55. Maestre, F. T. *et al.* Plant Species Richness and Ecosystem Multifunctionality in Global Drylands. *Science* **335**, 214–218 (2012).

56. Le Bagousse-Pinguet, Y. *et al.* Phylogenetic, functional, and taxonomic richness have both positive and negative effects on ecosystem multifunctionality. *Proc. Natl. Acad. Sci. U.S.A.* **116**, 8419–8424 (2019).

57. Cornelissen, J. H. C. *et al.* A handbook of protocols for standardised and easy measurement of plant functional traits worldwide. *Aust. J. Bot.* **51**, 335–380 (2003).

58. Pérez-Harguindeguy, N. *et al.* Corrigendum to: New handbook for standardised measurement of plant functional traits worldwide. *Aust. J. Bot.* **64**, 715–716 (2016).

59. Wright, I. J. *et al.* Global climatic drivers of leaf size. *Science* **357**, 917–921 (2017).

60. Deraison, H., Badenhausser, I., Börger, L. & Gross, N. Herbivore effect traits and their impact on plant community biomass: an experimental test using grasshoppers. *Functional Ecology* **29**, 650–661 (2015).

61. Cruz, P. *et al.* Leaf Traits as Functional Descriptors of the Intensity of Continuous Grazing in Native Grasslands in the South of Brazil. *Rangeland Ecology & Management* **63**, 350–358 (2010).

62. Salt, D. E., Baxter, I. & Lahner, B. Ionomics and the Study of the Plant Ionome. *Annu. Rev. Plant Biol.* **59**, 709–733 (2008).

951 63. Gaucherand, S. & Lavorel, S. New method for rapid assessment of the functional
952 composition of herbaceous plant communities. *Austral Ecology* **32**, 927–936 (2007).

953 64. Gross, N., Börger, L., Duncan, R. P. & Hulme, P. E. Functional differences between alien
954 and native species: do biotic interactions determine the functional structure of highly
955 invaded grasslands? *Functional Ecology* **27**, 1262–1272 (2013).

956 65. Siefert, A. *et al.* A global meta-analysis of the relative extent of intraspecific trait variation
957 in plant communities. *Ecology Letters* **18**, 1406–1419 (2015).

958 66. Schneider, C. A., Rasband, W. S. & Eliceiri, K. W. NIH Image to ImageJ: 25 years of image
959 analysis. *Nat Methods* **9**, 671–675 (2012).

960 67. Varley, J. A. A Textbook of Soil Chemical Analysis By P. R. Hesse London: John Murray
961 (1971), pp. 520, £7·50. *Experimental Agriculture* **8**, 184–184 (1972).

962 68. Kuo, S. Phosphorus. in *Methods of Soil Analysis* 869–919 (John Wiley & Sons, Ltd, 1996).
963 doi:10.2136/sssabookser5.3.c32.

964 69. Kettler, T. a., Doran, J. w. & Gilbert, T. l. Simplified Method for Soil Particle-Size
965 Determination to Accompany Soil-Quality Analyses. *Soil Science Society of America*
966 *Journal* **65**, 849–852 (2001).

967 70. Penone, C. *et al.* Imputation of missing data in life-history trait datasets: which approach
968 performs the best? *Methods Ecol Evol* **5**, 961–970 (2014).

969 71. Poyatos, R., Sus, O., Badiella, L., Mencuccini, M. & Martínez-Vilalta, J. Gap-filling a
970 spatially explicit plant trait database: comparing imputation methods and different levels of
971 environmental information. *Biogeosciences* **15**, 2601–2617 (2018).

972 72. Jetz, W. *et al.* Monitoring plant functional diversity from space. *Nature Plants* **2**, 1–5
973 (2016).

974 73. Swenson, N. G. Phylogenetic imputation of plant functional trait databases. *Ecography* **37**,
975 105–110 (2014).

976 74. Dinno, A. PARAN: Stata module to compute Horn's test of principal components/factors.
977 (2009).

978 75. Bueno, C. G. *et al.* Reply to: The importance of trait selection in ecology. *Nature* **618**, E31–
979 E34 (2023).

76. Laughlin, D. C. *et al.* Intraspecific trait variation can weaken interspecific trait correlations when assessing the whole-plant economic spectrum. *Ecology and Evolution* **7**, 8936–8949 (2017).

77. Brown, A., Butler, D. W., Radford-Smith, J. & Dwyer, J. M. Changes in trait covariance along an orographic moisture gradient reveal the relative importance of light- and moisture-driven trade-offs in subtropical rainforest communities. *New Phytologist* **236**, 839–851 (2022).

78. Delhaye, G. *et al.* Interspecific trait integration increases with environmental harshness: A case study along a metal toxicity gradient. *Functional Ecology* **34**, 1428–1437 (2020).

79. Cheverud, J. M., Wagner, G. P. & Dow, M. M. Methods for the Comparative Analysis of Variation Patterns. *Systematic Biology* **38**, 201–213 (1989).

80. Blonder, B. Hypervolume concepts in niche- and trait-based ecology. *Ecography* **41**, 1441–1455 (2018).

81. Blonder, B. *et al.* New approaches for delineating *n* -dimensional hypervolumes. *Methods Ecol Evol* **9**, 305–319 (2018).

82. Berdugo, M., Gaitán, J. J., Delgado-Baquerizo, M., Crowther, T. W. & Dakos, V. Prevalence and drivers of abrupt vegetation shifts in global drylands. *Proc. Natl. Acad. Sci. U.S.A.* **119**, e2123393119 (2022).

83. Berdugo, M., Kéfi, S., Soliveres, S. & Maestre, F. T. Plant spatial patterns identify alternative ecosystem multifunctionality states in global drylands. *Nature ecology & evolution* **1**, 0003 (2017).

84. Fong, Y., Huang, Y., Gilbert, P. B. & Permar, S. R. chngpt: threshold regression model estimation and inference. *BMC Bioinformatics* **18**, 454 (2017).

85. Schwarz, G. Estimating the Dimension of a Model. *The Annals of Statistics* **6**, 461–464 (1978).

86. Pinheiro, J. *et al.* Package 'nlme'. *Linear and nonlinear mixed effects models, version* **3**, 274 (2017).

87. Bates, D. *et al.* lme4: Linear Mixed-Effects Models using 'Eigen' and S4. (2024).

88. Maire, V. *et al.* Global effects of soil and climate on leaf photosynthetic traits and rates. *Global Ecology and Biogeography* **24**, 706–717 (2015).

89. K. Barton, MuMIn: Model Selection and Model Averaging Based on Information Criteria (AICc and alike) (R Package Version, 1–1, 2014).

90. Zuur, A. F., Ieno, E. N., Walker, N., Saveliev, A. A. & Smith , G. M. *Mixed Effects Models and Extensions in Ecology with R*. (Springer, 2009).

Acknowledgements

We thank the editor and the four referees for the constructive and positive comments during the revision of the paper. We acknowledge Sainbileg Undrakhbold, Munkhbat Uuganbayar, Batbold Byambatsogt, Sanchir Khaliun, Shijirbaatar Solongo, Bud Batchuluun, Michael Sloan, Sedona Spann, John Spence, Erika Geiger, Isys Souza, Richard Onoo, Thiago Araújo, Mancha Mabaso, Percy Mutseka Lunga, Louis Eloff, Julius Sebei, Dr Jorrie J. Jordaan, Dr Edwin Mudongo, Dr Vincent Mokoka, Baltimore Mokhou, Thabang Maphanga, Dr Dave Thompson (SAEON), Dr Anke S. K. Frank, Rose Matjea, Florian Hoffmann, Chris Goebel, Bruce Semple, Bobby Tamayo, Rebecca Peters, Adriana Lozada Piña, Roxana Ledezma, Eduardo Vidal, Franco Perona, Julio M. Alcántara, Armin Howell, Robin Reibold, Nick Melone, Megan Starbuck, Erika Geiger, Bush Heritage Australia, the University of Limpopo, Comunidad Agricola Quebrada de Talca, Conaf Chile, South African Environmental Observation Network (SAEON) for assistance with field work and plant identification, the South African Military for assistance with field work and/or granting access to their properties, and the Scientific Services Kruger National Park. This research was funded by the European Research Council (ERC Grant agreement 647038 1004 [BIODESERT]) and Generalitat Valenciana (CIDEGENT/2018/041). N.G. was supported by CAP 20-25 (16-IDEX-0001) and the AgreenSkills+ fellowship programme which 1020 has received funding from the EU's Seventh Framework Programme under grant agreement N° FP7-609398 (AgreenSkills+ contract). F.T.M. acknowledges support from the King Abdullah University of Science and Technology (KAUST), the KAUST Climate and Livability Initiative, the University of Alicante (UADIF22-74 and VIGROB22-350), the Spanish Ministry of Science and Innovation (PID2020-116578RB-I00), and the Synthesis Center (sDiv) of the German Centre for Integrative Biodiversity Research Halle–Jena–Leipzig (iDiv). Y.L.B.-P. was supported by a Marie Sklodowska-Curie Actions Individual Fellowship (MSCA-1018 IF) within the European Program Horizon 2020 (DRYFUN Project 656035). H.S. is supported by a María Zambrano fellowship funded by the Ministry of Universities and European Union-Next Generation plan. L.W. acknowledges support from the US National Science Foundation (EAR 1554894). G.M.W. acknowledges support from the Australian Research Council (DP210102593) and TERN. M.B is supported by a Ramón y Cajal grant from Spanish Ministry of Science (RYC2021-031797-I). LvdB and KT were supported by the German Research Foundation (DFG) Priority Program SPP-1803 (TI388/14-1). A.F. acknowledges the financial support from ANID PIA/BASAL FB210006 and Millenium Science Initiative Program NCN2021-050. A.J. was supported by the Bavarian Research

Alliance for travel and field work (BayIntAn UBT 2017 61). A.L. and L.K. acknowledge support from the German Research Foundation, DFG (grant CRC TRR228) and German Federal Government for Science and Education, BMBF (grants 01LL1802C and 01LC1821A). BB and SU were supported by the Taylor Family-Asia Foundation Endowed Chair in Ecology and Conservation Biology. PJR and AJM acknowledge support from Fondo Europeo de Desarrollo Regional through the FEDER Andalucía operative programme, FEDER-UJA 1261180 project. E.M.-J. and C.P. acknowledge support from the Spanish Ministry of Science and Innovation (PID2020-116578RB-I00). D.J.E was supported by the Hermon Slade Foundation. J.D. and A.Rodríguez acknowledge support from the FCT (2020.03670.CEECIND and SFRH/BDP/108913/2015, respectively), as well as from the MCTES, FSE, UE, and the CFE (UIDB/04004/2021) research unit financed by FCT/MCTES through national funds (PIDDAC). S.R. acknowledges support from the U.S. Department of Energy (DE-SC-0008168), U.S. Department of Defense (RC18-1322), and the U.S. Geological Survey Ecosystems Mission Area. Any use of trade, firm, or product names is for descriptive purposes only and does not imply endorsement by the U.S. government. EHS acknowledges support from Mexican National Science and Technology Council (CONACYT PN 5036 and 319059). A.N. and C.B. acknowledge the support from FCT - Fundação para a Ciência e a Tecnologia (CEECIND/02453/2018/CP1534/CT0001, PTDC/ASP-SIL/7743/ 2020, UIDB/00329/2020), from AdaptForGrazing project (PRR-C05-i03-I-000035) and from LTsER Montado platform (LTER_EU_PT_001). Field work of GP and JMZ was supported by UNRN (PI 40-C-873).

Author contributions

N.G., F.T.M., and Y.L.B.-P. conceived this study. F.T.M., N.G., and Y.L.B.-P. designed and coordinated the global field survey. N.G., P.L., and Y.L.B.-P. developed the original idea of the analyses presented in the manuscript, with inputs from F.T.M., M.B., R.M., M.D-B., V.M., E.M-J., H.S., S.S., and E.V.. F.J. developed the theoretical model on plant cover. Fieldwork was done by all co-authors with the assistance of M.G.G. for field site assessments. Laboratory analyses were done by V.O., B.G., S.A., C.P., M.G.G., and I.S.P. The trait database was built by N.G., R.M., and Y.L.B.-P. Data and code handling, curation, and verification were done by N.G, R.M. V.O., B.G., I.S.P., and Y.L.B.-P. Statistical analyses were performed by N.G., M.B., and R.M. N.G., Y.L.B.-P., and F.T.M. wrote the first manuscript draft and all authors worked on the final version.

Ethics declarations

Competing interests

The authors declare no competing interests.

Additional Information

Supplementary Information is available for this paper. Correspondence and requests for materials should be addressed to Nicolas Gross (nicolas.gross@inrae.fr), Fernando T. Maestre Gil (ft.maestre@gmail.com), Yoann Pinguet (yoann.pinguet@imbe.fr).

Extended Data Captions

Extended Data Figure 1. The trait space of global dryland rangelands. **a-c** represent the probabilistic species distributions in the space defined by a Principal Component Analysis (PCA) on whole-plant and leaf size, and on leaf chemical traits. **a** shows the dimensions related to plant size and leaf C-economy. **b-c** show the additional, but independent dimensions related to the plant elementome characterized by the concentration of 14 elements in plant leaves: C, N, P, Mg, Mn, Ca, Cu, Al, Ba, Fe, K, Na, S, and Zn. The dryland trait space displayed five major dimensions (Principal Components PC1 to PC5), accounting for 66.7 % of the total trait variation. In **a**, Leaf traits related to leaf C-economy (PC1) and plant size (PC3) varied along two orthogonal dimensions and accounted for a total of 28.2% of trait variation. In **b-c**, the plant elementome accounted for 55.5% of trait variation. While a dimension of the plant elementome covaried with the leaf C-economy dimension[27] (N-P-K on PC1), it also added three other orthogonal dimensions that were associated with important macro- and micronutrients (PC2, PC4, PC5). These findings show that a large fraction of trait diversity found across global drylands is not captured by plant size and leaf C-economy alone, but by the plant elementome (see Supplementary Figure 5 for an additional description of the elementome; Supplementary Figure 8 for the PCA ran without the gap-filling of the data; Supplementary Figure 7 for pictures of dryland plant species). The color gradient depicts the different species densities in the trait space (high and low density in red and fading yellow, respectively). The arrow length is proportional to the trait loadings. Each point represents the location of a species within the five-dimensional trait space for all the species surveyed (n = 1347). Abbreviations: maximum plant height, H; Lateral spread, LS; Leaf length, LL; leaf area, LA; specific leaf area, SLA; leaf dry matter content, LDMC. See also Supplementary Table 4 for detailed results.

Extended Data Figure 2. Aridity reshuffles the trait space of global dryland rangelands. We show how trait covariation changes along the aridity gradient using Principal Component Analysis (PCA) conducted for sites with aridity values located below and above the aridity threshold of ~0.7 (Low aridity n = 338; high aridity n = 1009). The arrow length is proportional to the loadings of the traits considered. In **a-b**, four principal components were selected at aridity values <0.7 while in **c-e** five components were selected at aridity values >0.7. See Extended Data Figure 1 for trait abbreviations and Supplementary Table 4 for detailed results.

Extended Data Figure 3. Presence of grazers modulates the trait space of global dryland rangelands. We show how trait covariation changes with increasing grazing pressure using Principal Component analysis (High Grazing *n* = 382; Medium Grazing *n* = 410; Low Grazing *n* = 389; Ungrazed *n* = 166). The arrow length is proportional to the loadings of the traits considered. In **a-i**, five principal components were significantly selected in low, medium, and high grazing pressures. In **j-k**, four principal components were significantly selected in ungrazed plots. See Extended Data Figure 1 for trait abbreviations and Supplementary Table 6 for detailed results. Low = low grazing pressure, Med = medium grazing pressure, and High = high grazing pressure.

Extended Data Figure 4. Representation of the trait hypervolume before and after crossing the ~0.7 aridity threshold. We show the 2D projection of the hypervolume for each pair of PCA dimensions shown in Extended Data Figure 1 (n-dimensions = 5, from PC1 to PC5). Colored dots represent the locations of each measured species within the trait space. The blue and the red large bright dots represented the centroids of each hypervolume before and after an aridity value of 0.7 (low aridity *n* = 189; high aridity *n* = 696). Colored lines show the 0.95 confidence intervals of the hypervolume before and after this aridity value.

Extended Data Figure 5. Response of elemental concentration in soils (the soil elementome) to aridity. Soil elements covary across the 326 sampled plots along a unique Principal Component axis (PC1) that account for 65.8 % of soil total variation (see Methods). **a** shows responses of the soil elementome, illustrated using the soil PC 1, to aridity. PC1 shows a quadratic response to aridity with non-linear decrease occurring only in the most arid areas, i.e., those with aridity values > 0.8. Grazing did not modify this response. **b** shows how the soil elementome responded to aridity using a sliding windows analysis (see methods). We first ordered the 326 plots according to their aridity level. We then defined an aridity window that represented 10% of the global aridity gradient and selected all plots within this aridity range (n > 30 plots in each window). We finally examined how the bootstrapped covariation of soil elements across plots changed as aridity increased. We found that aridity further increased the covariation of soil elements in the most arid rangelands surveyed. See Supplementary Table 7 for detailed results of model selections evaluating the response of the soil elementome to aridity. Error band shows the 0.95 confidence interval in **a** and **b**.

Extended Data Figure 6. Global decrease in plant cover driven by aridity and grazing. a shows the averaged model parameters (± 0.95 confidence interval) for different predictors (i.e. aridity, grazing, soil, and geographical variables) on plant cover (n = 326 plots). Significant predictors do not cross the vertical dotted line. Aridity and grazing were the main drivers of plant cover. **b** illustrates the effects of aridity on plant cover. Vertical dashed and dotted lines represent the mean location of the threshold and its 0.95 confidence interval, respectively. Error band shows the 0.95 confidence interval. **c** shows grazing effect on plant cover (High Grazing n = 98; Medium Grazing n = 97; Low Grazing n = 88; Ungrazed n = 43). Data are represented as boxplots where the middle line is the median, the lower and upper hinges correspond to the first and third quartiles, the upper and lower lines show the 0.95 confidence interval. Data beyond the confidence interval are outlying points that are plotted individually. We tested whether different grazing pressure levels showed significant differences using a generalized least squares model ($p < 0.001$). Letters show results of a post-hoc test based on bootstrapped pairwise comparisons between grazing pressure levels. Different letters indicate significant differences among grazing pressure levels. Plant cover decreased non-linearly at aridity ~0.7 and was the lowest under high grazing pressure.

Extended Data Figure 7. Plant cover mediates the effect of aridity and grazing pressure on trait diversity across global dryland rangelands. **a-b** show the response of trait diversity (hypervolume and trait covariation respectively) to plant cover using a sliding window procedure (see Methods). Increasing plant cover decreased hypervolume and increased trait covariations, with a significant threshold value occurring at a plant cover value close to 50% ± CI (vertical dashed lines, the dotted lines show its 0.95 percentile Confidence Interval, CI). See Supplementary Table 8 for detailed results of model selection evaluating the response of the plant elementome to plant cover. Error band shows the 0.95 confidence interval in **a** and **b**.

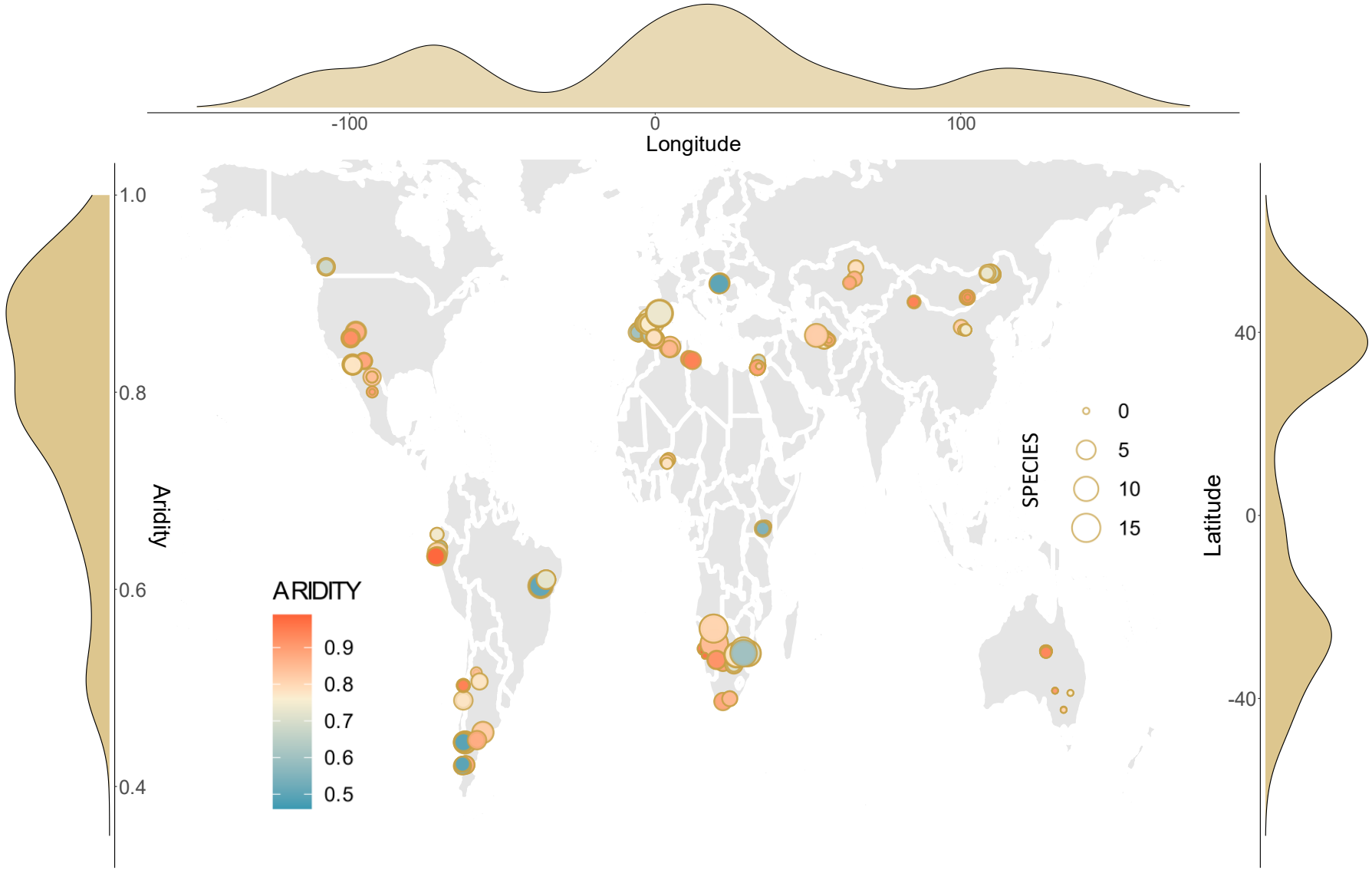
-100
0
100
Longitude
1.0
0.8
0.6
0.4
Aridity
ARIDITY
0.9
0.8
0.7
0.6
0.5
SPECIES
0
5
10
15
40
0
-40
Latitude

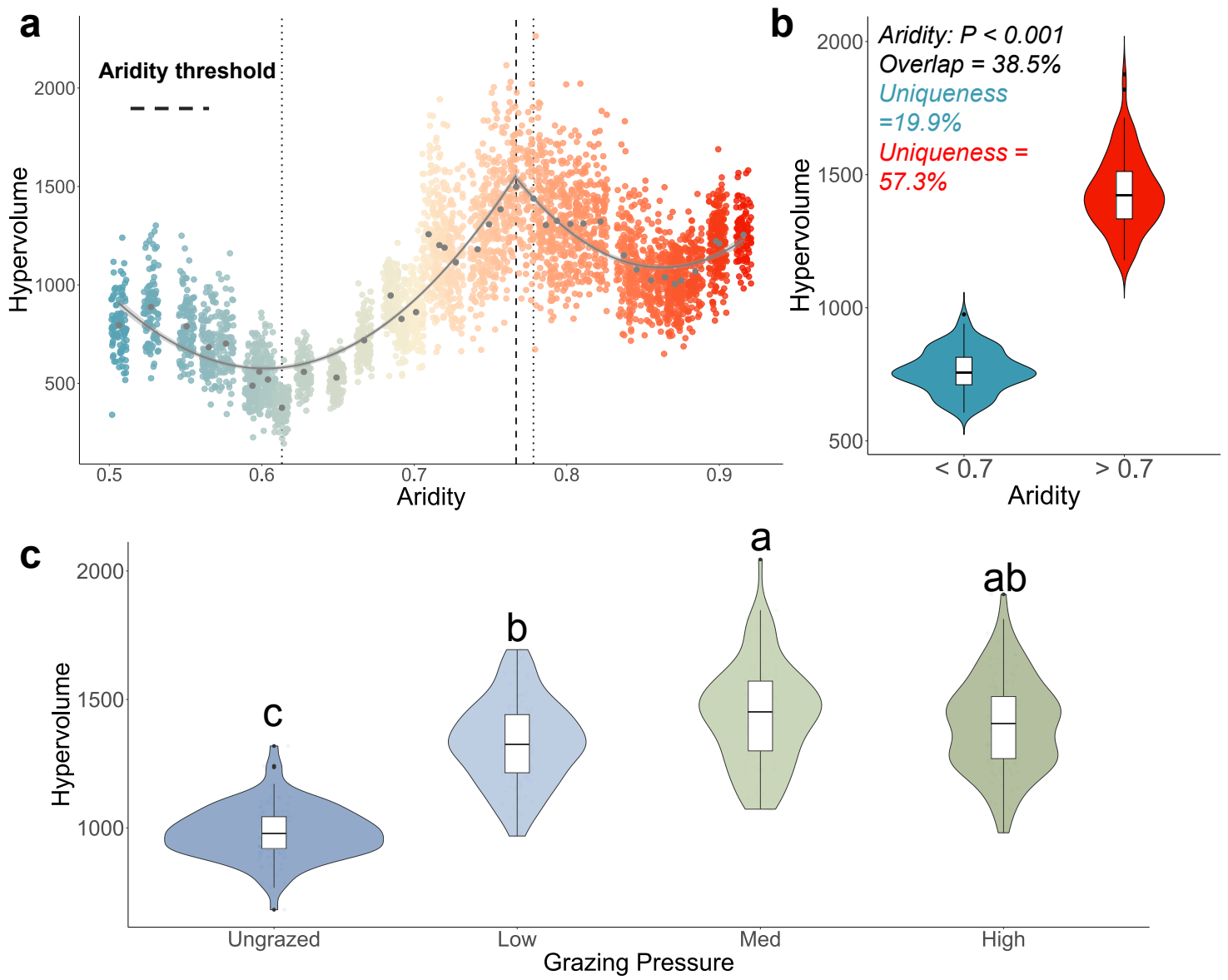
a
Aridity threshold
Hypervolume
2000
1500
1000
500
0.5
0.6
0.7
0.8
0.9
Aridity
b
Aridity: P < 0.001
Overlap = 38.5%
Uniqueness =19.9%
Uniqueness = 57.3%
Hypervolume
2000
1500
1000
500
< 0.7
> 0.7
Aridity
c
Hypervolume
2000
1500
1000
c
b
a
ab
Ungrazed
Low
Med
High
Grazing Pressure

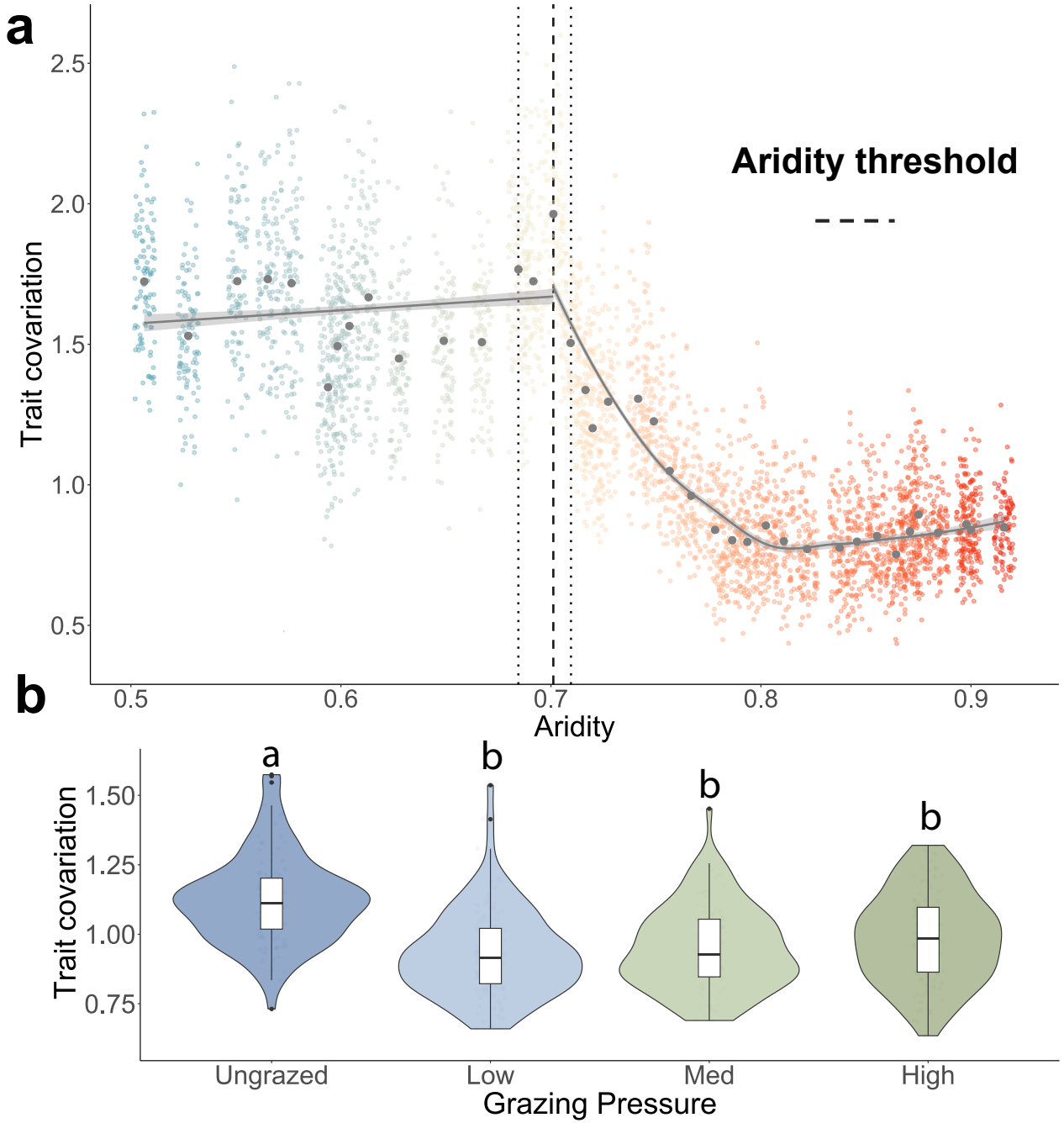
a
Trait covariation
2.5
2.0
1.5
1.0
0.5
Aridity threshold
0.5
0.6
0.7
0.8
0.9
Aridity
b
Trait covariation
1.50
1.25
1.00
0.75
a
b
b
b
Ungrazed
Low
Med
High
Grazing Pressure

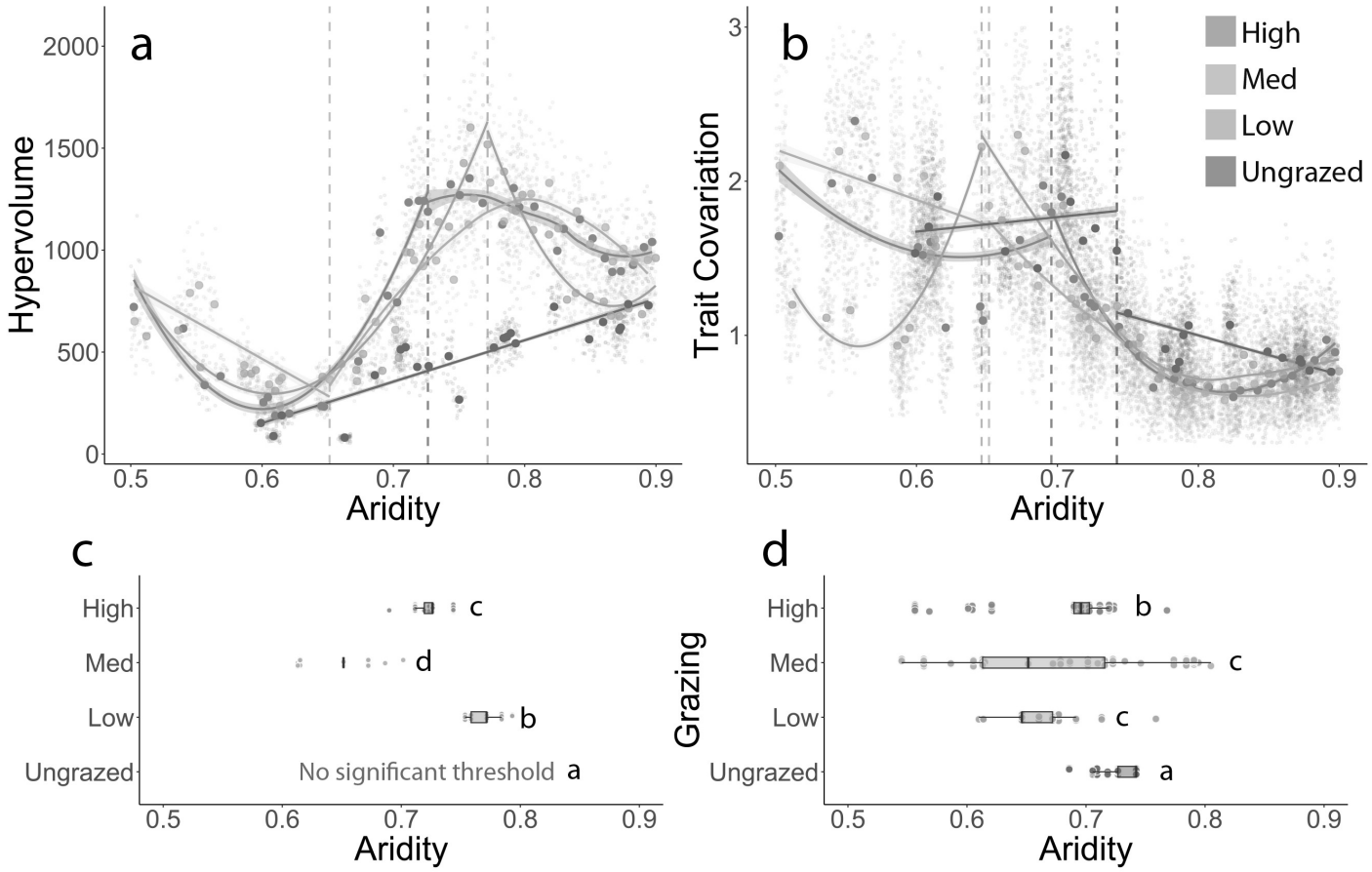
a
Hypervolume
2000
1500
1000
500
0
0.5
0.6
0.7
0.8
0.9
Aridity
b
Trait Covariation
3
2
1
High
Med
Low
Ungrazed
Aridity
c
High
Med
Low
Ungrazed
c
d
b
No significant threshold
a
Aridity
d
Grazing
High
Med
Low
Ungrazed
b
c
c
a
Aridity